Modified Lucas-Washburn theory for fluid filling in nanotubes

Mohammad Heiranian and Narayana R. Aluru

Phys. Rev. E **105**, 055105 — Published 16 May 2022

DOI: 10.1103/PhysRevE.105.055105

Modified Lucas-Washburn Theory for Fluid Filling in Nanotubes

Mohammad Heiranian[1] and Narayana R. Aluru[2*]

[1]*Department of Chemical and Environmental Engineering, Yale University, New Haven, Connecticut 06520-8286, United States*

[2]*Oden Institute for Computational Engineering and Sciences, Walker Department of Mechanical Engineering, The University of Texas at Austin, Austin, TX 78712 USA*

Revised on 4/25/2022

Ultrafast water transport in carbon nanotubes (CNTs) has drawn a great deal of attention in a number of applications, such as water desalination, power generation and biomolecule detection. With the recent experimental advances in water filling of isolated CNTs, the Lucas-Washburn theory for capillary rise in tubes needs to be revisited for a better understanding of the physics and dynamics of water filling in CNTs. Here, the Lucas-Washburn theory is corrected for the hydrodynamic entrance effects and variation of capillary pressure and hydrodynamic properties with the radius and length of CNTs. Due to the large slippage in CNTs, inclusion of the entrance effects is important particularly for the initial stages of filling where a $L \propto t$ scaling, as opposed to $L^2 \propto t$, is observed in our molecular dynamics (MD) simulations. The corrected Lucas-Washburn theory is shown to predict the water filling dynamics in CNTs as observed in MD simulations. With the corrected theory, we achieve a better understanding of capillary rise and water filling dynamics in CNTs.

Keywords: Capillary Rise, Filling dynamics, Nanopores, Graphene, Carbon Nanotubes, Nanofluidics, Water, Hydrodynamics, Slip Length, Viscosity

---

* Corresponding Author, e-mail: aluru@utexas.edu web: http://sites.utexas.edu/aluru/

INTRODUCTION

When confined in nanopores and nanochannels, water is found to possess unique properties that differ substantially from those of bulk water[1,2]. For example, the out of plane dielectric constant of water has recently been observed to be significantly lower, compared to the bulk value, when confined in graphene slit channels[3,4]. As another example, giant water flow rates have been observed in carbon nanotubes (CNTs) owing to the highly frictionless surfaces[5-9]. Water transport in CNTs has been studied for the past two decades, where enhancement factors (flow rates normalized by the rates predicted using the classical no-slip Hagen–Poiseuille (HP) equation) of the order of 1000 have been reported[6,10,11]. Recently, Secchi et al.[12] experimentally measured water flow rates in individual CNTs where a massive slip length of ~300 nm was reported for a 15 nm-diameter CNT. This massive slip length contradicts the values obtained from the classical molecular dynamics (MD) simulations (usually in the range of 70 nm-120 nm). Secchi et al.[12] suggest that the unique electronic structure of the CNT confinement possibly leads to the observation of the unexpectedly large slip lengths. While electronic structure effects are certainly important in CNTs, the accuracy of the underlying theory used to extract slip lengths from experimental data is also important. Since the hydrodynamic resistance inside CNTs is negligible compared to the entrance/exit resistance, estimation of slip lengths from experimentally measured flow rates strongly depends on the accuracy of the theory used to describe the entrance/exit flow[13,14]. For example, using a corrected Sampson theory[14] to describe the entrance/exit flow, the experimentally measured flow rates by Secchi et al.[12] lead to slip lengths comparable to those obtained from MD simulations. Therefore, the need for accurate theories describing flow in nanopores is of particular interest. Recently, water filling of isolated CNTs has been investigated[15], where the spatial presence of water along a single CNT is reported by a shift in the measured

Raman radial breathing modes. Given these advances[15-19], accurate theoretical models are required for a thorough understanding of the water capillary rise in CNTs from experiments.

Dynamics of capillary flow in circular tubes was first investigated within the framework of classical fluid mechanics about a century ago[20-22]. Edward W. Washburn introduced an equation for fluid meniscus dynamics in the capillary by integrating the HP velocity of penetration equation where the driving pressure on the fluid is set to be the Laplace capillary pressure $\left(\frac{2\sigma cos\theta}{R}\right)$, i.e.,

$$L^2 = \frac{\sigma cos\theta}{2\mu}(R + 4b)t \quad (1)$$

where L is the height of the penetrating meniscus, t is the transient time, R is the tube radius, θ is the contact angle of the meniscus with the tube wall, μ is the fluid viscosity, σ is the fluid surface tension and b is the slip length. See Figure 1a for the definition of L, R and θ. Equation (1), however, has been found to be inaccurate for some nanoscale flows (e.g., capillary rise in CNTs) possibly due to the deviations of fluid interfacial properties at nanoscale as observed in molecular dynamics simulations[23-30]. For example, Supple et al.[25] found that the Lucas-Washburn (LW) equation in (1) cannot describe capillary filling dynamics in CNTs as the meniscus height is proportional to time ($L \propto t$) in their simulations. In another MD study[24], the filling rate of nanotubes was found to be slower than the rate predicted from the LW equation. The slower filling rate was also observed by Martic et al.[26] where a velocity-dependent contact angle was introduced to correct the LW equation. Effects of dynamic contact angles, inertia forces, slip lengths, and viscosity variation in gel pores of cement-based materials were also considered in other recent studies[31,32] for modifying LW equation. Cai et al.[33,34] provided a comprehensive review on LW equation modifications and extensions for porous media. For nanotubes (e.g., CNTs) with large slip lengths, MD simulations showed that the entrance effects must be considered as the early stage

of filling is dominated by the viscous dissipation at the entrance[23,27]. Here, we revisit the original Lucas-Washburn equation for water capillary rise in CNTs and account for the hydrodynamic entrance effects by incorporating the recently corrected-Sampson theory into the capillary rise equation. Capillary pressure is also modified for tubes with small diameters as the Laplace capillary pressure is likely to fail for small pores[33]. Additionally, we incorporate the variation of viscosity and slip length with radius and length of CNTs. The corrected Lucas-Washburn (CLW) equation is able to describe the filling rate of CNTs from MD simulations where $L \propto t$ and $L \propto \sqrt{t}$ laws are observed for short-time and long-time fillings, respectively. Water slip lengths for different sizes of CNTs are also estimated from LW, CLW, and other methods. Unlike those from LW, slip lengths from CLW match the values expected from MD simulations.

CORRECTED LUCAS-WASHBURN THEORY

Ultrafast water flow inside CNTs has been observed by both experimental and computational studies due to the frictionless nature of the interface[7,35,36]. This ultralow hydrodynamic resistance inside CNTs leads to the dominance of entrance hydrodynamic resistance for finite-length CNTs. Therefore, the recently corrected Sampson (CS) theory[14] for the entrance resistance is included in the total hydrodynamic resistance as follows:

$$R_{\text{total}} = R^{\text{CS}}_{\text{entrance}} + R^{\text{HP}}_{\text{CNT}} . \tag{2}$$

where $R^{\text{CS}}_{\text{entrance}} = \frac{C_{\text{CS}}\,\mu}{2R^3}$ and $R^{\text{HP}}_{\text{CNT}} = \frac{8\mu L}{\pi(R^4+4bR^3)}$ are, respectively, the corrected Sampson resistance for the entrance (excluding the exit resistance by the $\frac{1}{2}$ factor) and Hagen-Poiseuille resistance inside the CNTs. C_{CS} is the pre-factor in the corrected Sampson equation. Values of C_{CS} for different pore radii can be obtained from the expressions given in Ref.[14] where slip lengths inside single-layer graphene nanopores, which appear in the C_{CS} expressions, are also provided.

Variation of μ and b with the radius and length are considered using the recently corrected HP (CHP) theory presented in Ref.[13]. Total resistance in the left-hand side of equation (2) is obtained from the driving capillary pressure and volumetric flow rate $\left(R_{\text{total}} = \frac{\Delta P}{Q}\right)$. Capillary pressure is given by[37]

$$\Delta P = \left(2 + \frac{\delta r}{r}\right)\frac{\sigma cos\theta}{R} \tag{3}$$

where r is the radius of the curvature of the meniscus and δr is an infinitesimal change in the radius. See the Supplementary Information for the derivation of equation (3). For large-diameter tubes, $\frac{\delta r}{r}$ is negligible reducing equation (3) to $\Delta P = \frac{2\sigma cos\theta}{R}$ which is the Laplace capillary pressure used in the original Lucas-Washburn equation. However, for small-diameter CNTs, δr and r may be comparable. Therefore, equation (3) is modified as,

$$\Delta P = \frac{C_{\text{cp}}\sigma cos\theta}{R} \tag{4}$$

where C_{cp} is defined as the capillary pre-factor ($C_{\text{cp}} \geq 2$) which changes with pore radius. Note that $C_{\text{cp}} = 2$ in the original Lucas-Washburn equation. Here, we model the capillary pre-factor as $C_{\text{cp}} = 2 + \left(\frac{0.3\text{nm}}{R}\right)^{1.6}$, where 0.3 nm indicates the approximate size of a single water molecule and R is expressed in nanometers (see the Supplementary Information for more details).

Neglecting inertia forces and using equations (2), (4), and $R_{\text{total}} = \frac{\Delta P}{Q}$, the rate of penetration can be written as

$$\frac{dL}{dt} = \frac{2C_{\text{cp}}\sigma\cos\theta(R+4b)}{\pi C_{\text{CS}}\mu(R+4b)+16\mu L}. \tag{5}$$

Integrating equation (5), the corrected Lucas-Washburn equation is given by

$$t = \frac{\pi C_{\mathrm{cs}} \mu}{2 C_{\mathrm{cp}} \sigma \cos\theta} L + \int_0^L \frac{8\mu(z) z}{C_{\mathrm{cp}} \sigma \cos\theta (R + 4b(z))} dz \quad (6)$$

where z is the axial coordinate of the tube as shown in Figure 1a. Previously, it was shown that the slip length varies along the tube $b(z)$ for very short CNTs[13]. Assuming a constant slip length, constant viscosity, a C_{cp} pre-factor of 2 and neglecting the first term, equation (6) reduces to the original LW equation (see equation (1)). The first term in equation (6) is due to the entrance effects and follows the $L \propto t$ scaling which was observed in some previous studies. The $L \propto t$ scaling dominates the filling dynamics for short-time (or short-length) filling. For long-time (or long-length) filling, the second term in equation (6) dominates the filling. Assuming a constant slip length b and viscosity μ for long-time filling, the first term in equation (6) (entrance effects) can be neglected for $L \gg \frac{\pi C_{\mathrm{cs}}}{8}(R + 4b)$ where the filling dynamics follows $L \propto \sqrt{t}$ scaling. The condition reduces to $L \gg \frac{\pi C_{\mathrm{cs}}}{2} b$ for small-radius CNTs as the slip length is much larger than the radius ($b \gg R$).

WATER STRUCTURE AND DYNAMICS OF FILLING FROM MD SIMULATIONS

All-atom MD (AAMD) simulations have been performed to study the structure and dynamics of capillary rise in CNTs. As shown in Figure 1b, each simulation box consists of water molecules, a graphene sheet at the entrance and a CNT. In each graphene sheet, a nanopore with a size similar to the diameter of the CNT is drilled. (10,10), (14,14), (18,18), (26,26) and (34,34) CNTs with the center-to-center diameters of 1.36 nm, 1.90 nm, 2.44 nm, 3.53 nm and 4.61 nm are considered in this study. The simulation box dimensions vary from 6.3 nm to 20.01 nm in *x* and *y*, and 100 nm to 400 nm in *z*. Different dimensions in *x* and *y* are used to account for the porosity of the nanopores (the ratio of pore area to membrane area is <0.042). The systems contain about 326,000-783,000

136 atoms of which about 200,000-300,000 atoms are the reservoir water molecules initially placed
137 next to the graphene sheets. Note that the schematic of the simulation box in Figure 1b is truncated
138 for a better presentation. See the Methods section and Supplementary Information, for more details
139 about MD simulations.

140 Water contact angles are calculated geometrically from the MD simulations by first obtaining
141 the water densities averaged for different rectangular slabs placed in each CNT[38-40] (see the
142 Supplementary Information). The region with the sharp reduction in density indicates the boundary
143 of the meniscus (liquid-vapor interface). The cosine of the contact angles are reported for different
144 CNT radii in Figure 2a. The cosine of the contact angles increases with increasing radius from
145 0.125 ($\theta = 82.8^{o}$) for the (10,10) CNT to 0.180 ($\theta = 79.6^{o}$) for the (34,34) CNT. For very large
146 radii, the cosine of the angles is expected to converge to that of the limiting case of a single-layer
147 graphene (0.53 or $\theta = 58^{o}$) for the carbon-water interaction parameters[38] employed in this study
148 (see the methods section). As the contact angle increases for smaller radii, the surface becomes
149 more hydrophobic due to the enhanced confinement in smaller CNTs.

150 In Figure 2b, normalized water density as a function of the normalized radial distance from the
151 CNT center is plotted for the different CNTs considered in this study. Water density layering is
152 observed near the wall of CNTs where the density can reach about 3 times the bulk water density.
153 Water density reaches that of the bulk water in the center of CNTs except for the small CNTs (e.g.,
154 (10,10) CNT) where the density layering regions are overlapped with no bulk-like region. The
155 velocity distribution in the radial direction (Figure 2c) exhibits plug-like flow profiles with velocity
156 jumps at the interfacial region of CNTs. These velocity profiles are similar to flow profiles
157 observed in pressure driven flows. In Figure 2c, one might argue that the velocity should increase
158 for smaller radii as the slip length is larger. Although this may be true for pressure-driven flows

(assuming a fixed external pressure for all radii), it is not the case here since the capillary pressure decreases for small radii (e.g., velocities in (14,14) and (10,10) CNTs are lower than those of other larger CNTs). This can also be confirmed by examining equation (5) where the penetration velocity decreases with decreasing $\cos\theta$ for small radii.

DYNAMICS OF FILLING FROM THE CORRECTED LUCAS-WASHBURN THEORY

Extensive MD simulations have been carried out to report the penetration length of the meniscus as a function of simulation time for all CNT sizes considered in this study (see Figure 3). Since the simulations involve a large number of atoms and the capillary rise is a slow process, simulating filling dynamics is limited to filling lengths of about 45 nm-150 nm depending on the diameter of the CNTs. The MD results are used as the reference to examine the accuracy of the corrected model (equation (6)) compared to the original LW theory (equation (1)). As mentioned in the previous sections, slip length and viscosity for the CLW equation are obtained from Ref.[13] where the variation of viscosity $\mu(L,R)$ and friction coefficient $\lambda(L,R)$ with length and radius of CNT are given. Slip length can simply be obtained from $\bar{b}(L,R)=\frac{\mu(L,R)}{\lambda(L,R)}$. For a given radius, $\bar{b}(L)$ is a CNT length-averaged slip length (considering that slip length in the entrance region of the CNT differs from that of the middle section of the CNT). However, slip length at a given point along the CNT, $b(z)$, is required in equation (6). Therefore, we discretize the entire length of the CNT with a uniform mesh, $z_n=\frac{\text{Total length}}{N}n$ and $n=1,2,\dots,N$. The slip length at any point z_n can then be written as $b_n=n\bar{b}_n-(b_1+b_2+\cdots+b_{n-1})$ for $n\geq 2$. $b_1=\bar{b}_1$ for $n=1$. The same can be applied to the viscosity inside the CNTs. However, as discussed in the Supplementary Information, we observed that the length-variation of viscosity does not significantly change the filling dynamics (i.e., for simplicity, one can use the values of water viscosity for an infinity-long CNTs).

The corrected Sampson pre-factor is given in Ref.[14] as it changes depending on the radius and slippage at the graphene nanopore. The surface tension of water is taken to be 0.072 N/m. Capillary pre-factor for different CNTs is obtained from $C_{\mathrm{cp}} = 2 + \left(\frac{0.3\mathrm{nm}}{R}\right)^{1.6}$. Note that for $R > \sim 1$ nm, we can simply use a constant pre-factor $C_{\mathrm{cp}} = 2$ (see the Supplementary Information). All the parameters used in equation (6) are tabulated in TABLE 1.

As shown in Figure 3, the CLW theory is able to match the meniscus penetration displacement with time obtained from MD simulations. The initial filling of CNTs follows a nearly linear scaling, $L \propto t$, indicating the importance of accounting for the entrance effects in the model. However, one should note that the filling dynamics cannot be approximated solely by the Sampson equation (entrance resistance) as suggested by Gravelle et al.[23] since the dependence of L on t starts to deviate from the $L \propto t$ scaling in the subsequent stages of filling (Figure 3 and Figure S8 of the Supplementary Information). The LW theory, where a constant slip length is assumed in equation (1), fails to predict the filling dynamics in CNTs mainly because the entrance effects are ignored (the filling dynamics always obeys the $L^2 \propto t$ law in LW theory). For long-length or long-time filling where the entrance effects can be ignored (e.g., for lengths much larger than $L \gg \frac{\pi C_{\mathrm{cs}}}{2} b = 102$ nm in (10,10) CNTs), CLW and LW result in similar filling dynamics assuming that, in the LW equation, slip length and viscosity for infinitely long CNTs, contact angles from MD simulations, and modified capillary pre-factors for small-diameter CNTs are considered (see Supplementary Information).

PREDICTING SLIP LENGTHS FROM FILLING DYNAMICS IN CNTS

Accurate estimation of slip lengths in CNTs from the experimentally measured flow rates is of particular interest in the nanofluidic community. Lack of accurate theories (Sampson and HP

theories) has been suggested as one of the possible explanations for the estimated giant slip lengths from the experimental pressure-driven flow rates reported by Secchi et al[12]. Recently, with the advances in detecting water molecules spatially along isolated CNTs[15], dynamics of capillary rise, obtained from experiments, could potentially be used to estimate the slip lengths of water in CNTs. Slip lengths can be determined from LW and CLW theories (equations (1) and (6)), given that the filling rates are available from experiments or computational simulations. For the CLW theory, the CNT-length dependent slip length $b(z)$ can be solved for numerically by using a uniform mesh along the CNT. In Figure 4, slip length as a function of CNT radius for different CNT lengths is plotted from different theories, simulations, and experiments. The corrected HP theory, which is based on MD simulations, is used to generate the reference slip length data. Flow rates from the CHP theory have been shown to compare well with the rates from MD simulations and experiments in the previous study[13]. The filling dynamics in Figure 3 is used to predict the slip lengths from LW and CLW theories for the CNT radii considered in this work. As expected, the slip lengths from the CLW theory follow the trend obtained from the CHP. The original LW theory underestimates the slip lengths for short and small-radius CNTs. This is because entrance effects, viscosity variation with CNT size and capillary pre-factor variation with radii are important for shorter and smaller CNTs. The slips lengths from LW and CLW theories, however, become comparable for longer and larger-diameter CNTs. Most of the slip length measurements from experiments and simulations are for μm-long and infinitely-long CNTs. The estimated slip lengths are widely scattered where the slip lengths range from ~10 nm to 450,000 nm. These discrepancies are possibly due to the inaccurate theories used to estimate slip lengths, lack of accurate forcefields for the interaction between water and CNTs, challenging experimental flow rate measurements and effects of defects and contaminants in experiments. We should note that we used the force-

field developed by Wu et al.[38] which results in comparable water contact angles on graphene with the experimental values.

CONCLUSION

The Lucas-Washburn theory was revisited and corrected for the hydrodynamic entrance effects and variation of capillary pressure and hydrodynamic properties for nanometer scale pores. The effect of the entrance resistance, modeled by the corrected Sampson theory[14], is important for initial stages of filling (i.e., short-time or short-length filling) as well as for tubes with large slip lengths. The capillary pressure is predicted to decrease slightly as radius of CNTs decreases (nanometer-radius CNTs). Effect of the variation of viscosity and slip length on filling dynamics is significant for short and small-radius CNTs. The corrected theory is able to predict the water filling dynamics in CNT from MD simulations. For the initial stages of filling, a $L \propto t$ scaling is observed due to the effects of the entrance resistance. $L^2 \propto t$ scaling is expected for long-length or long-time stages of filling similar to the filling dynamics obtained from the original Lucas-Washburn theory.

METHODS

MD simulations were carried out using the LAMMPS package.[41] The features of simulation boxes (Figure 1b) were discussed in the Water Structure and Dynamics of Filling from MD Simulations section. We used the SPC/E water model and the SHAKE algorithm to maintain the rigidity of the water molecule. The interactions between carbon atoms and water molecules were modeled by the force-field parameters given in Wu *et al*.[38] The carbon atoms are frozen in space. We note that freezing the carbon atoms can affect the flow rates up to 10%-20% [7,42]. The LJ cutoff distance was 12 Å. The long range electrostatic interactions were computed by the Particle-

Particle-Particle-Mesh (PPPM) method.[43] Periodic boundary conditions were applied in all the three directions. In the *z* direction, the simulation box is separated from its images by large vacuum regions (see the Supplementary Information). For each system, the energy of the system was first minimized for 10000 steps. Next, the water reservoir was equilibrated using NPT ensemble for 1 ns at a pressure of 1 atm and a temperature of 300 K with a time-step of 1fs. The NPT simulations allow the water molecules to reach the bulk water equilibrium density (1 g/cm^3). Then, NVT simulations were performed for 2 ns to further equilibrate the systems. Temperature was maintained at 300 K by using the Nosè-Hoover thermostat with a time constant of 0.1 ps.[44,45] In the equilibrium simulations, a graphene sheet with no pore is used to solely equilibrate water molecules without penetrating the tube. The final production simulations were performed in NVT ensemble for up to 12 ns to study the capillary rise in CNTs.

ACKNOWLEDGEMENT

This work was supported as part of the Center for Enhanced Nanofluidic Transport (CENT), an Energy Frontier Research Center funded by the U.S. Department of Energy, Office of Science, Basic Energy Sciences under Award # DE-SC0019112. The simulations were performed using the Extreme Science and Engineering Discovery Environment (XSEDE) (supported by National Science Foundation (NSF) Grant No. OCI1053575) and Blue Waters (supported by NSF awards OCI-0725070, ACI-1238993 and the state of Illinois).

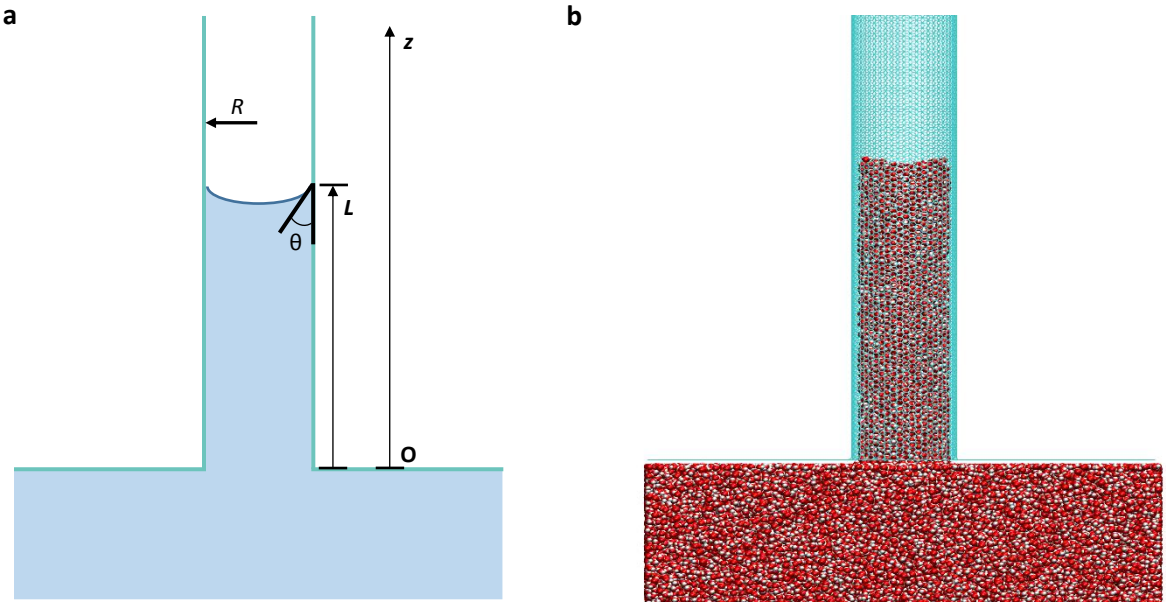

Figure 1. a) Schematic of capillary filling of a CNT is shown. Radius (*R*), water contact angle (θ) and filling length (*L*) of the CNT are illustrated. *z* is the axial coordinate along the CNT. The CNT and graphene walls are shown in cyan and water is shown in light blue. **b)** A typical simulation system for a (26,26) CNT (*R*=1.76 nm) is shown for the simulation time of ~1 nanosecond. The carbon, oxygen and hydrogen atoms are presented in cyan, red and white, respectively. The simulation box is truncated for a better presentation.

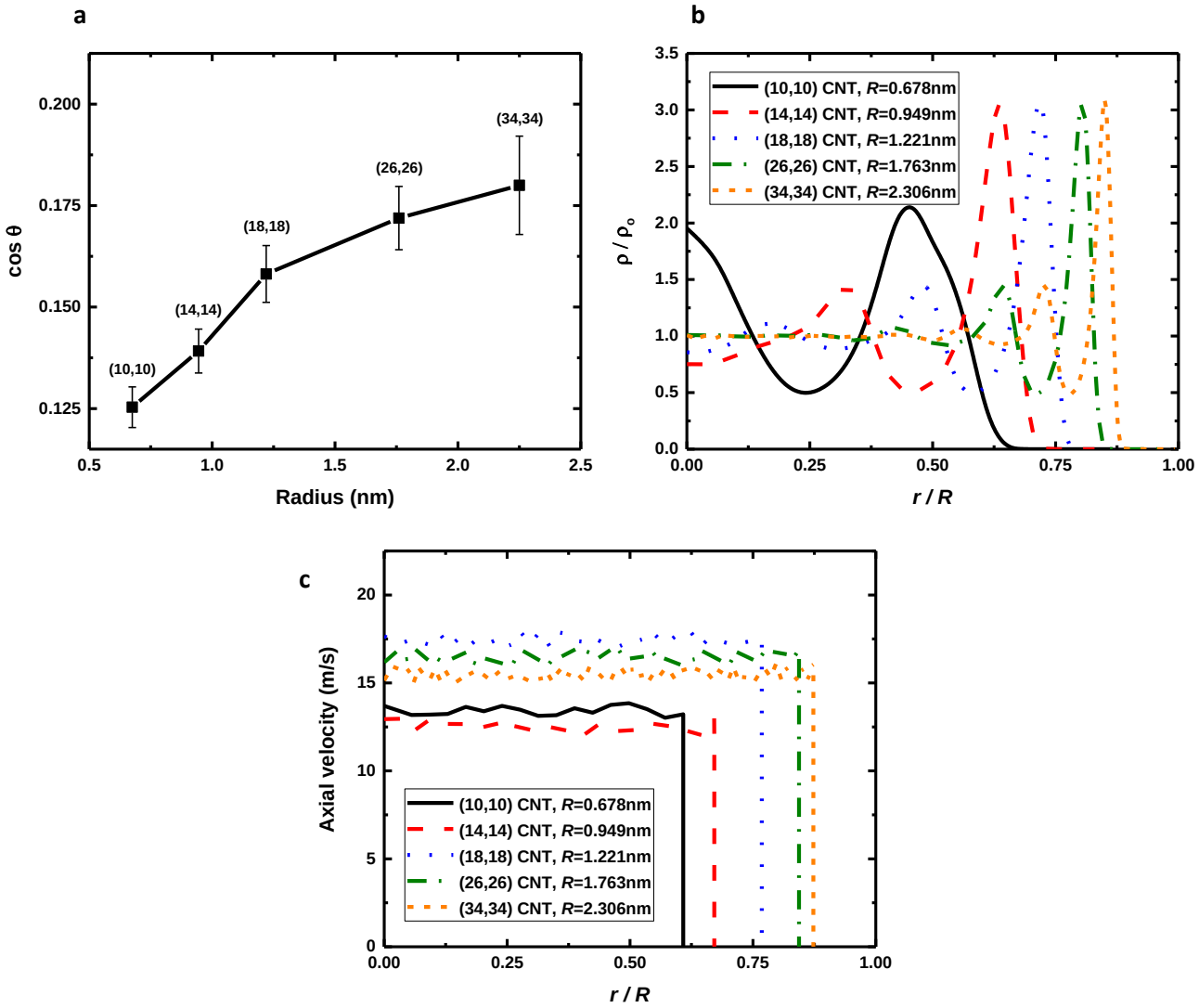

Figure 2. a) Cosines of water contact angles for the different CNTs considered in this study. The cosine of contact angle increases with increasing radius. It is expected to reach the cosine of contact angle on a flat graphene for very large CNT radii. **b)** Water density distribution (normalized by the bulk water density) in the radial direction (normalized by the CNT radius) for the different CNTs considered in this study. **c)** Axial velocity of water molecules as a function of the normalized radial distance from the center of CNTs. The water velocity is calculated for the CNT filling in the time interval of 1900ps-2100ps. For both density and velocity calculations, we consider the water molecules that are 1 nm away from the pore entrance and the meniscus surface

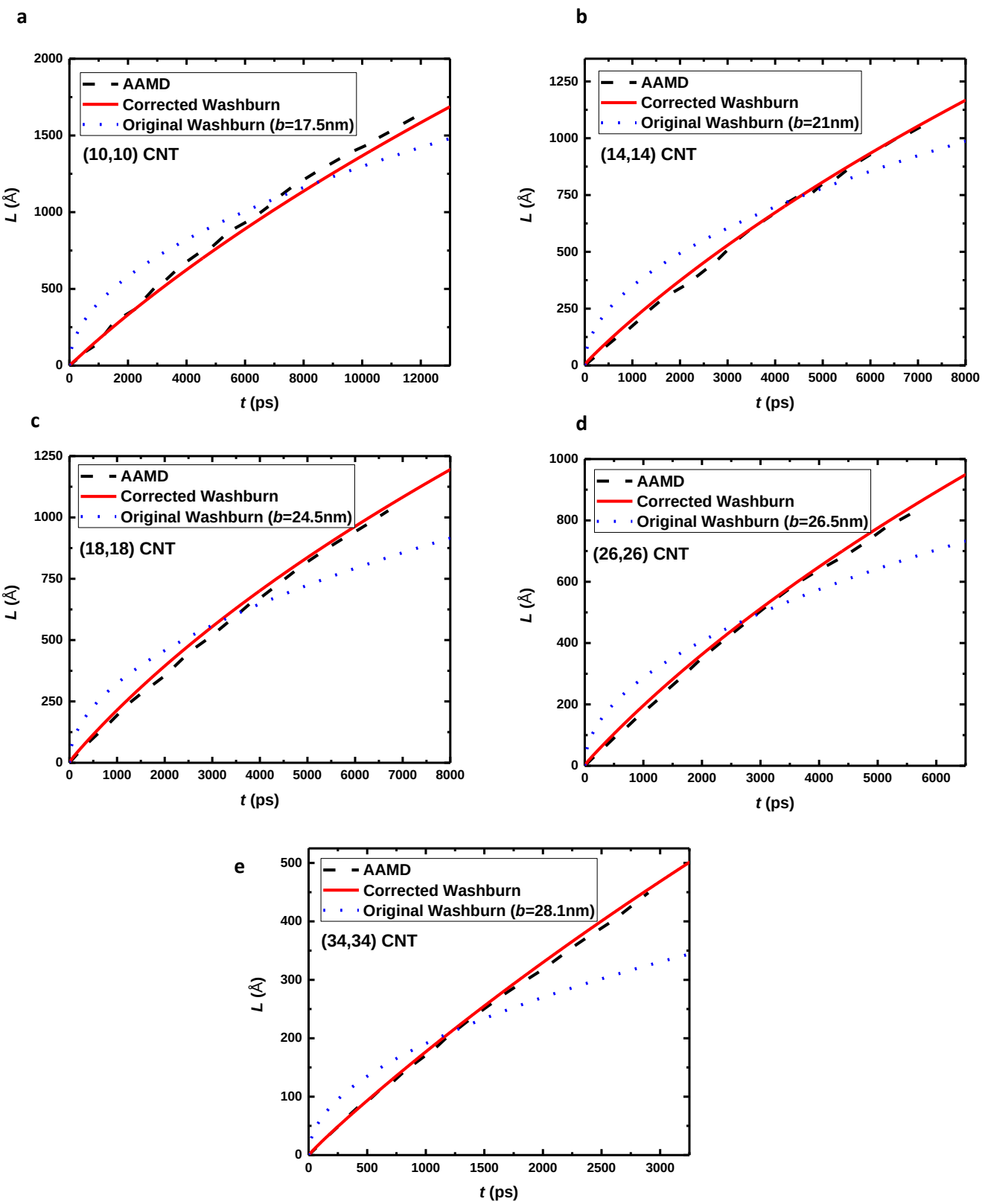

Figure 3. The length of the CNTs filled with water as a function of time from all-atom MD simulations is compared with the filling lengths predicted by the corrected Washburn (CLW) theory and the original

Washburn (LW) theory for **a)** (10,10), **b)** (14,14), **c)** (18,18), **d)** (26,26), and **e)** (34,34) CNTs. The corrected Washburn theory is able to describe the filling dynamics well compared to that of the AAMD simulations. The original Washburn theory, however, fails as it does not account for the hydrodynamic entrance effects, slip length and viscosity variations with CNT length and radius, as well as the corrected capillary pressure in nanometer-diameter CNTs. In the original LW theory, viscosity is taken as 0.85 mPa·s which is the water bulk viscosity. The slip length in the original LW theory is chosen such that we obtain the best possible match with the data from MD simulations. We note that slip lengths based on infinitely-long CNTs lead to a massive overestimation of filling rates by the original LW theory (see Figure S8a of the Supplementary Information).

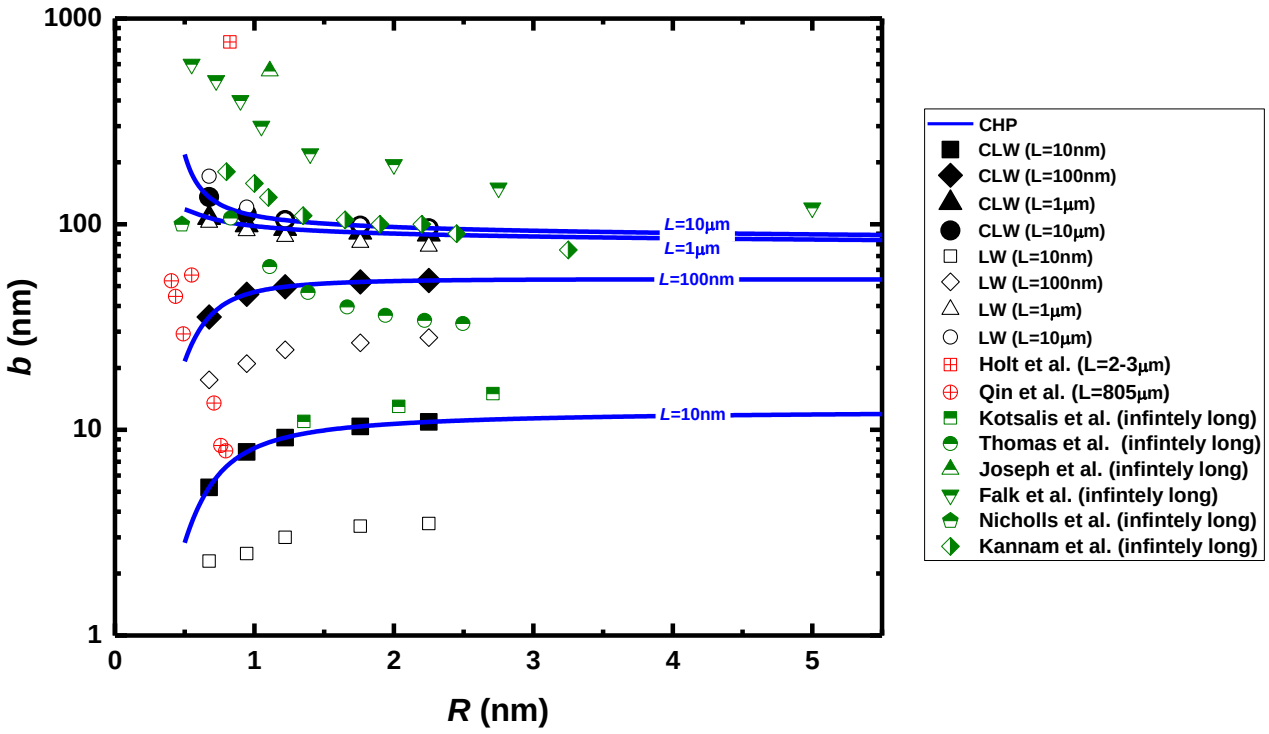

Figure 4. Slip lengths as a function of radius of CNTs with different tube lengths predicted by different theories (corrected Hagen-Poiseuille theory (CHP, blue curve), corrected Lucas-Washburn theory (CLW, filled black symbols) and original Lucas-Washburn theory (LW, hollow black symbols)). The CHP model, which is based on MD simulations, is used as the reference here. The LW theory fails to predict the slip lengths for short and small-radius CNTs. As both length and radius increase, LW and CLW theories result in identical slip lengths since the effects of hydrodynamic entrance, viscosity variation and nano-capillary pressure vanish. Experimental[5,6,46] and computational[7,35,47-50] data (shown by red and green symbols, respectively) shows how wide the range of slip lengths are in the literature. In other notable experiments by Majumder et al[5]. and Du et al[51]. (not shown in the Figure), very high slip lengths of 39000nm-68000nm and 485000nm are reported, respectively.

TABLE 1 The parameters used in the CLW model (equation (6)) for different CNT sizes. Slip length and viscosity vary along the tube length. The resulting filling dynamics are plotted in Figure 3.

Cases	C_{CS}	C_{cp}	σ (N/m)	$\cos\theta$
(10,10) CNT	0.465	2.27	0.072	0.125
(14,14) CNT	0.480	2.15	0.072	0.139
(18,18) CNT	0.495	2.10	0.072	0.158
(26,26) CNT	0.630	2.05	0.072	0.172
(34,34) CNT	0.780	2.03	0.072	0.180

REFERENCES

1 Koga, K., Gao, G. T., Tanaka, H. & Zeng, X. C. Formation of ordered ice nanotubes inside carbon nanotubes. *Nature* **412**, 802-805, doi:10.1038/35090532 (2001).

2 Mashl, R. J., Joseph, S., Aluru, N. R. & Jakobsson, E. Anomalously immobilized water: A new water phase induced by confinement in nanotubes. *Nano Letters* **3**, 589-592, doi:10.1021/nl0340226 (2003).

3 Motevaselian, M. H. & Aluru, N. R. Universal reduction in dielectric response of confined fluids. *Acs Nano* **14**, 12761-12770, doi:10.1021/acsnano.0c03173 (2020).

4 Fumagalli, L. *et al.* Anomalously low dielectric constant of confined water. *Science* **360**, 1339-1342, doi:10.1126/science.aat4191 (2018).

5 Majumder, M., Chopra, N., Andrews, R. & Hinds, B. J. Nanoscale hydrodynamics - Enhanced flow in carbon nanotubes. *Nature* **438**, 44-44, doi:10.1038/43844a (2005).

6 Holt, J. K. *et al.* Fast mass transport through sub-2-nanometer carbon nanotubes. *Science* **312**, 1034-1037, doi:10.1126/science.1126298 (2006).

7 Joseph, S. & Aluru, N. R. Why are carbon nanotubes fast transporters of water? *Nano Letters* **8**, 452-458, doi:10.1021/nl072385q (2008).

8 Hummer, G., Rasaiah, J. C. & Noworyta, J. P. Water conduction through the hydrophobic channel of a carbon nanotube. *Nature* **414**, 188-190, doi:10.1038/35102535 (2001).

9 Farimani, A. B., Heiranian, M. & Aluru, N. R. Nano-electro-mechanical pump: Giant pumping of water in carbon nanotubes. *Scientific Reports* **6**, 1-6, doi:10.1038/srep26211 (2016).

10 Thomas, J. A. & McGaughey, A. J. H. Water flow in carbon nanotubes: Transition to subcontinuum transport. *Physical Review Letters* **102**, 184502, doi:10.1103/PhysRevLett.102.184502 (2009).

11 Thomas, J. A. & McGaughey, A. J. H. Reassessing fast water transport through carbon nanotubes. *Nano Letters* **8**, 2788-2793, doi:10.1021/nl8013617 (2008).

12 Secchi, E. *et al.* Massive radius-dependent flow slippage in carbon nanotubes. *Nature* **537**, 210-213, doi:10.1038/nature19315 (2016).

13 Heiranian, M. & Aluru, N. R. Nanofluidic transport theory with enhancement factors approaching one. *Acs Nano* **14**, 272-281, doi:10.1021/acsnano.9b04328 (2020).

14 Heiranian, M., Taqieddin, A. & Aluru, N. R. Revisiting Sampson's theory for hydrodynamic transport in ultrathin nanopores. *Physical Review Research* **2**, 043153, doi:10.1103/PhysRevResearch.2.043153 (2020).

15 Faucher, S. *et al.* Diameter dependence of water filling in lithographically segmented isolated carbon nanotubes. *ACS Nano* **15**, 2778-2790, doi:10.1021/acsnano.0c08634 (2021).

16 Agrawal, K. V., Shimizu, S., Drahushuk, L. W., Kilcoyne, D. & Strano, M. S. Observation of extreme phase transition temperatures of water confined inside isolated carbon nanotubes. *Nat. Nanotechnol.* **12**, 267-273, doi:10.1038/nnano.2016.254 (2017).

17 Cambre, S., Schoeters, B., Luyckx, S., Goovaerts, E. & Wenseleers, W. Experimental observation of single-file water filling of thin single-wall carbon nanotubes down to chiral index (5,3). *Physical Review Letters* **104**, 207401, doi:10.1103/PhysRevLett.104.207401 (2010).

18 Fagan, J. A. *et al.* Separation of empty and water-filled single-wall carbon nanotubes. *ACS Nano* **5**, 3943-3953, doi:10.1021/nn200458t (2011).

19 Wenseleers, W., Cambre, S., Culin, J., Bouwen, A. & Goovaerts, E. Effect of water filling on the electronic and vibrational resonances of carbon nanotubes: Characterizing tube opening by Raman spectroscopy. *Adv. Mater.* **19**, 2274-2278, doi:10.1002/adma.200700773 (2007).

20 Lucas, R. Ueber das Zeitgesetz des kapillaren Aufstiegs von Flüssigkeiten. *Kolloid-Zeitschrift*, 15-22 (1918).

21 Washburn, E. W. The dynamics of capillary flow. *Physical Review* **17**, 273-283, doi:10.1103/PhysRev.17.273 (1921).

22 Bosanquet, C. H. On the flow of liquids into capillary tubes. *Philosophical Magazine* **45**, 525-531, doi:10.1080/14786442308634144 (1923).

23 Gravelle, S., Ybert, C., Bocquet, L. & Joly, L. Anomalous capillary filling and wettability reversal in nanochannels. *Physical Review E* **93**, 033123, doi:10.1103/PhysRevE.93.033123 (2016).

24 Vo, T. Q., Barisik, M. & Kim, B. Near-surface viscosity effects on capillary rise of water in nanotubes. *Physical Review E* **92**, 053009, doi:10.1103/PhysRevE.92.053009 (2015).

25 Supple, S. & Quirke, N. Rapid imbibition of fluids in carbon nanotubes. *Physical Review Letters* **90**, 214501, doi:10.1103/PhysRevLett.90.214501 (2003).

26 Martic, G. *et al.* A molecular dynamics simulation of capillary imbibition. *Langmuir* **18**, 7971-7976, doi:10.1021/la020068n (2002).

27 Joly, L. Capillary filling with giant liquid/solid slip: Dynamics of water uptake by carbon nanotubes. *J. Chem. Phys.* **135**, 214705, doi:10.1063/1.3664622 (2011).

28 Chen, C. *et al.* A many-body dissipative particle dynamics study of spontaneous capillary imbibition and drainage. *Langmuir* **26**, 9533-9538, doi:10.1021/la100105f (2010).

29 Schebarchov, D. & Hendy, S. C. Dynamics of capillary absorption of droplets by carbon nanotubes. *Physical Review E* **78**, 046309, doi:10.1103/PhysRevE.78.046309 (2008).

30 Dimitrov, D. I., Milchev, A. & Binder, K. Capillary rise in nanopores: Molecular dynamics evidence for the Lucas-Washburn equation. *Physical Review Letters* **99**, 054501, doi:10.1103/PhysRevLett.99.054501 (2007).

31 Wang, P. *et al.* Atomistic insights into cesium chloride solution transport through the ultra-confined calcium-silicate-hydrate channel. *Physical Chemistry Chemical Physics* **21**, 11892-11902, doi:10.1039/c8cp07676f (2019).

32 Hou, D. S. *et al.* Modified Lucas-Washburn function of capillary transport in the calcium silicate hydrate gel pore: A coarse-grained molecular dynamics study. *Cement and Concrete Research* **136**, 106166, doi:10.1016/j.cemconres.2020.106166 (2020).

33 Cai, J. C. *et al.* Lucas-Washburn equation-based modeling of capillary-driven flow in porous systems. *Langmuir* **37**, 1623-1636, doi:10.1021/acs.langmuir.0c03134 (2021).

34 Jianchao Cai, B. X., Liang Luo, Zhien Zhang. *Chapter 43 - Analysis of Spontaneous Imbibition in Carbon Nanotube, Handbook of Nanomaterials for Industrial Applications*. 793-798 (Elsevier, 2018).

35 Falk, K., Sedlmeier, F., Joly, L., Netz, R. R. & Bocquet, L. Molecular origin of fast water transport in carbon nanotube membranes: Superlubricity versus curvature dependent friction. *Nano Letters* **10**, 4067-4073, doi:10.1021/nl1021046 (2010).

36 Celebi, K. *et al.* Ultimate permeation across atomically thin porous graphene. *Science* **344**, 289-292, doi:10.1126/science.1249097 (2014).

37 Glover, P. W. J. *Petrophysics*. (University of Aberdeen, UK, 2000).

38 Wu, Y. B. & Aluru, N. R. Graphitic carbon-water nonbonded interaction parameters. *J. Phys. Chem. B* **117**, 8802-8813, doi:10.1021/jp402051t (2013).

39 Werder, T., Walther, J. H., Jaffe, R. L., Halicioglu, T. & Koumoutsakos, P. On the water-carbon interaction for use in molecular dynamics simulations of graphite and carbon nanotubes. *J. Phys. Chem. B* **107**, 1345-1352, doi:10.1021/jp0268112 (2003).

40 Heiranian, M., Wu, Y. B. & Aluru, N. R. Molybdenum disulfide and water interaction parameters. *Journal of Chemical Physics* **147**, 104706, doi:10.1063/1.5001264 (2017).

41 Plimpton, S. Fast parallel algorithms for short-range molecular-dynamics. *J. Comput. Phys.* **117**, 1-19, doi:10.1006/jcph.1995.1039 (1995).

42 Sam, A., Kannam, S. K., Hartkamp, R. & Sathian, S. P. Water flow in carbon nanotubes: The effect of tube flexibility and thermostat. *J. Chem. Phys.* **146**, 234701 doi:10.1063/1.4985252 (2017).
43 Darden, T., York, D. & Pedersen, L. Particle mesh Ewald: An *N*.log(*N*) method for Ewald sums in large systems. *J. Chem. Phys.* **98**, 10089-10092, doi:10.1063/1.464397 (1993).
44 Nose, S. A unified formulation of the constant temperature molecular-dynamics methods. *J. Chem. Phys.* **81**, 511-519 (1984).
45 Hoover, W. G. Canonical dynamics - equilibrium phase-space distributions. *Phys. Rev. A* **31**, 1695-1697, doi:10.1103/PhysRevA.31.1695 (1985).
46 Qin, X. C., Yuan, Q. Z., Zhao, Y. P., Xie, S. B. & Liu, Z. F. Measurement of the rate of water translocation through carbon nanotubes. *Nano Letters* **11**, 2173-2177, doi:10.1021/nl200843g (2011).
47 Kotsalis, E. M., Walther, J. H. & Koumoutsakos, P. Multiphase water flow inside carbon nanotubes. *International Journal of Multiphase Flow* **30**, 995-1010, doi:10.1016/j.ijmultiphaseflow.2004.03.009 (2004).
48 Thomas, J. A., McGaughey, A. J. H. & Kuter-Arnebeck, O. Pressure-driven water flow through carbon nanotubes: Insights from molecular dynamics simulation. *International Journal of Thermal Sciences* **49**, 281-289, doi:10.1016/j.ijthermalsci.2009.07.008 (2010).
49 Nicholls, W. D., Borg, M. K., Lockerby, D. A. & Reese, J. M. Water transport through carbon nanotubes with defects. *Molecular Simulation* **38**, 781-785, doi:10.1080/08927022.2011.654205 (2012).
50 Kannam, S. K., Todd, B. D., Hansen, J. S. & Daivis, P. J. How fast does water flow in carbon nanotubes? *J. Chem. Phys.* **138**, 094701, doi:10.1063/1.4793396 (2013).
51 Du, F., Qu, L. T., Xia, Z. H., Feng, L. F. & Dai, L. M. Membranes of vertically aligned superlong carbon nanotubes. *Langmuir* **27**, 8437-8443, doi:10.1021/la200995r (2011).